



# New insights into the GDF9-Hedgehog-GLI signaling pathway in human ovaries: from fetus to postmenopause

Parinaz Asiabi<sup>1</sup> · Clara David<sup>1</sup> · Alessandra Camboni<sup>1</sup> · Etienne Marbaix<sup>2</sup> · Marie-Madeleine Dolmans<sup>1,3</sup> · Christiani A. Amorim<sup>1</sup>

Received: 10 December 2020 / Accepted: 18 March 2021 / Published online: 26 March 2021

© The Author(s), under exclusive licence to Springer Science+Business Media, LLC, part of Springer Nature 2021

## Abstract

**Research question** Are glioma-associated oncogene homolog 1, 2, and 3 (GLI1, 2, and 3) and protein patched homolog 1 (PTCH1) specific markers for precursor theca cells in human ovaries as in mouse ovaries?

**Design** To study the GDF9-HH-GLI pathway and assess whether GLI1 and 3 and PTCH1 are specific markers for precursor theca cells in the human ovary, growth differentiation factor 9 (GDF9), Indian Hedgehog (IHH), Desert Hedgehog (DHH), Sonic Hedgehog (SHH), PTCH1 and GLI1, 2 and 3 were investigated in fetal ( $n=9$ ), prepubertal ( $n=9$ ), reproductive-age ( $n=15$ ), and postmenopausal ( $n=8$ ) human ovarian tissue. Immunohistochemistry against GDF9, IHH, DHH, SHH, PTCH1, GLI1, GLI2, and GLI3 was performed on human ovarian tissue sections fixed in 4% formaldehyde and embedded in paraffin. Western blotting was carried out on extracted proteins from the same samples used in the previous step to prove the antibodies' specificity. The quantitative real-time polymerase chain reaction was performed to identify mRNA levels for *Gdf9*, *Ihh*, *Gli1*, *Gli2*, and *Gli3* in menopausal ovaries.

**Results** Our results showed that, in contrast to mice, all studied proteins were expressed in primordial follicles of fetal, prepubertal, and reproductive-age human ovaries and stromal cells of reproductive-age and postmenopausal ovaries. Intriguingly, *Gdf9*, *Ihh*, and *Gli3* mRNA, but not *Gli1* and 2, was detected in postmenopausal ovaries. Moreover, GLI1, GLI3, and PTCH1 are not limited to a specific population of cells. They were spread throughout the organ, which means they are not specific markers for precursor theca cells in human ovaries.

**Conclusion** These results could provide a basis for understanding how this pathway modulates follicle development and ovarian cell steroidogenesis in human ovaries.

**Keywords** Growth differentiation factor 9 · Hedgehog ligands · PTCH1 receptor · Precursor theca cells · Glioma-associated oncogene homolog 1 · 2 · and 3

## Introduction

While orchestrated communication between the pituitary gland and the ovary is needed for reproduction in mammals, successful follicle growth and ovulation require highly

elaborate communication between the oocyte and its surrounding granulosa and theca cells. Any flaw in this process can have dire consequences on female reproductive health and fertility [1–3].

Theca cells play a crucial role in successful folliculogenesis by providing structural support and producing androstenedione as a substrate for granulosa cells to convert into estradiol [4]. Despite the importance of theca cells, their origin in the ovary has not been positively identified. There are studies in neonatal mouse ovaries showing that precursor theca cells can be detected by glioma-associated oncogene homolog 1 (GLI1) [3], GLI3, and protein patched homolog 1 (PTCH1) [5]. Cells positive for these markers differentiate into theca interna cells (TICs) in the presence of Hedgehog (HH) ligands synthesized by granulosa cells. Differentiated TICs express GLI1 [3], GLI2, PTCH2, and luteinizing hormone receptor (LHR) [5].

✉ Christiani A. Amorim  
christiani.amorim@uclouvain.be

<sup>1</sup> Pôle de Recherche en Gynécologie, Institut de Recherche Expérimentale et Clinique, Université Catholique de Louvain, Avenue Mounier 52, bte B1.52.02, 1200 Brussels, Belgium

<sup>2</sup> Gynecology and Andrology Department, Cliniques Universitaires Saint-Luc, 1200 Brussels, Belgium

<sup>3</sup> Pathology Department, Cliniques Universitaires Saint-Luc, Brussels, Belgium

For this process to occur, the HH pathway is activated in granulosa cells by secreted growth differentiation factor 9 (GDF9) expressed by oocytes [3]. Indeed, it has been reported that in mutant mice lacking GDF9, the TIC layer fails to develop, causing follicle development arrest at preantral stages [3, 6]. GDF9 has been shown to mediate induction and activation of the HH signaling pathway in neonatal mouse ovarian granulosa cells [3].

HH proteins are responsible for lineage specification in many organs [7], particularly mouse follicles, but HH ligands, Desert Hedgehog (DHH), and Indian Hedgehog (IHH) produced by granulosa cells are involved in the recruitment of TICs from the ovarian stroma [8, 9]. Moreover, DHH and IHH deletion studies in mice ovaries [3] and Leydig cells in testes [10] indicate that they are implicated in regulating the differentiation and steroidogenic capacity of endocrine cells, including TICs, partly by modulating the expression of *Sf-1/Nr5a1* and steroidogenic enzymes like cytochrome P450 family 11 subfamily A member 1 (*Cyp11a1*) and cytochrome P450 17A1 (*Cyp17a1*) (3, 10, reviewed by 11).

In mammalian ovarian follicles, the HH signaling pathway is activated by stoichiometric binding of HH ligands in granulosa cells to their receptor PTCH1 [12–14] on theca cells and their precursors [3, 9]. PTCH1 is a conserved 12-pass transmembrane protein receptor that plays an obligate negative regulatory role in the HH signaling pathway [15]. In the absence of HH proteins, PTCH1 suppresses constitutive activity in the seven-transmembrane G protein-like Smoothed (SMO) receptor [16]. The presence of HH proteins inactivates the action of PTCH1 in adjacent cells [17] by removing PTCH1 inhibition on SMO activity [16, 18, 19]. This leads to activation of latent cytoplasmic transcription factors, namely zinc finger proteins GLI1, 2 and 3 [17, 20], in (precursor) theca, interstitial/fibroblast, and/or perivascular cells within the theca layer [9, 21]. These transcription factors regulate the expression of selected genes, such as enzymes involved in the steroidogenic pathway of TICs, including *Cyp11a1* and *Cyp17a1* [9, 11].

Due to a lack of knowledge on the origin of TICs in human ovaries, the goal of this study was to investigate the GDF9-HH-GLI pathway in human ovaries and assess whether GLI1, 2, and 3 and PTCH1 are specific markers for precursor TICs, as has been demonstrated in mice [3, 5]. To this end, we analyzed the expression of proteins and genes involved in the GDF9-HH-GLI pathway in fetal, prepubertal, reproductive-age, and postmenopausal human ovaries.

## Materials and methods

### Collection of human ovarian samples

The Institutional Review Board approved the use of the human ovarian cortex of the Université Catholique de Louvain

on May 13, 2019 (IRB reference 2012/23MAR/125, registration number B403201213872). Thanks to the collaboration between UCLouvain's Gynecology Research Unit (GYNE) and the Anatomic Pathology Department of Saint-Luc's Hospital, we were able to study human ovarian biopsies obtained from the biobank of the Cliniques Universitaires Saint-Luc (BB190044). Based on the absence of ovarian pathologies (patient history) and anomalies and alterations (histological analysis), ovarian tissue fragments from fetal, prepubertal, reproductive-age, and postmenopausal ovaries (Table 1) were selected from the hospital biobank, where all samples of tissues/organs collected from patients are registered and stored. Apart from menopausal tissue, all ovaries contained follicles at different stages of development, as well as corpora lutea.

### Histological and immunohistochemical analyses

Excised biopsies were fixed in 4% formaldehyde (VWR, Leuven, Belgium) for 24 h before being dehydrated and embedded in paraffin. Paraffin blocks were serially sectioned (5- $\mu$ m-thick sections) (Microtome HM325, Thermo Fisher Scientific, Merelbeke, Belgium), and every tenth section was stained with hematoxylin and eosin (Merck, Darmstadt, Germany) for morphological analysis, while the remaining sections (Superfrost® Plus, Menzel-Glaser, Braunschweig, Germany) were kept for immunohistochemistry (IHC). Follicles were classified according to their stage of development as follows:

- Type 1: Resting primordial follicles containing a single layer of flattened granulosa cells
- Type 2: Primary follicles with one layer of cuboidal granulosa cells
- Type 3: Secondary follicles with two layers of granulosa cells
- Type 4: Secondary follicles with three or more layers of granulosa cells and the start of theca cell layer formation
- Type 5: Small antral follicles (less than 6 mm in diameter)
- Type 6: Large antral follicles (more than 6 mm in diameter)

IHC analysis was performed with GDF9, IHH, DHH, Sonic Hedgehog (SHH), PTCH1, GLI1, GLI2, and GLI3 antibodies on consecutive tissue sections using an indirect peroxidase method concurrently for all ages. Information on primary antibodies, their dilution and incubation time, and details about the different steps of IHC for each antibody are provided in Supplementary Table 1.

Briefly, tissue sections were deparaffinized and rehydrated, followed by endogenous peroxidase inhibition using hydrogen peroxide. Apart from GDF9, antigen retrieval was done in a water bath at 96°C for 20 min or 98°C for 75 min, depending

**Table 1** Number of used paraffin block samples and their age range

	Fetal	Prepubertal	Fertile	Menopausal
Age range	14–39 weeks	Newborn to 6 years	35–43 years	68–91 years
Number of samples*	9	9	15	8

\* Each sample corresponds to a patient

on the antibody. Nonspecific protein inhibition was performed using Tris-buffered saline (TBS), 3% non-fat milk, 7.5% bovine serum albumin, 1.5% Tween 20, and 3% human immunoglobulins (Igs, 3%, Sandoz, West Princeton, USA) before incubation with primary antibody. Secondary antibody incubation (60 min) with EnVision anti-mouse (Dako, USA) for PTCH1 and GLI1, and EnVision anti-rabbit (Dako, USA) for GDF9, IHH, DHH, SHH, GLI2, and GLI3 followed by streptavidin/horseradish peroxidase (HRP), was accomplished after overnight incubation with primary antibody. For negative controls, the primary antibody was omitted. Instead, in these slides, the FLEX negative control mouse cocktail of mouse IgG1, IgG2a, IgG2b, IgG3, and IgM ready-to-use (Dako Autostainer/Autostainer Plus, ref. IS750, Dako) and rabbit immunoglobulin fraction of serum from non-immunized rabbits, solid-phase absorbed ready-to-use (Dako Autostainer/Autostainer Plus, ref. IS600, Dako) depending on the primary antibody was added. Ovarian tissue and the same tissue used for positive controls were treated similarly, but without any primary antibody. Diaminobenzidine (DAB, Vector, Burlingame, USA) was used to stain the sections, followed by counterstaining with hematoxylin, dehydration in isopropanol, and mounting for further analyses.

### Scanning and image analyses

Stained sections were digitized with an SCN400 slide scanner (Leica Biosystems, Wetzlar, Germany) at 20× magnification. Using ImageJ software (version 1.52a, Wayne Rasband, NIH, USA), the total number of immunostained follicles for all proteins of interest was counted in each group (fetal, prepubertal, reproductive-age, and postmenopausal). Follicles were considered positive when staining was detected in the cytoplasm or nucleus of oocytes, granulosa, and/or theca cells. We finally identified all positive follicles at every stage of development in each age group and for each protein (Tables 2, 3, and 4). All ovarian tissue sections were scored for the intensity of staining in oocytes and granulosa, theca, and stromal cells. Relative intensities of staining were scored as follows: -, no staining; +, moderate staining; or ++, strong staining [21]. Immunostaining was evaluated blindly by two observers.

### Protein extraction

The Qproteome FFPE kit (Qiagen, Hilden, Germany) was used to extract proteins from formalin-fixed paraffin-

embedded (FFPE) tissue (fetal,  $n=4$ ; prepubertal,  $n=3$ ; reproductive-age,  $n=4$ ; postmenopausal,  $n=2$ ; positive controls,  $n=5$  ( $n$  corresponds to the number of the paraffin blocks, which represent individual samples)). Positive controls were the same samples as used for IHC (Supplementary Table 1). Extraction was achieved according to the kit datasheet. Briefly, the first step involves deparaffinization, where tissue sections (10–15- $\mu$ m thickness) are successively incubated for 10 min at room temperature (RT) in xylene and 100%, 96%, and 70% ethanol. After incubation, the supernatant is carefully removed and the pellet is retained. Once the paraffin has been removed, tissue sections undergo an incubation step for protein extraction. Samples are incubated in 100- $\mu$ l extraction buffer (EXB +  $\beta$ -mercaptoethanol) and undergo a first heating treatment using a heating block at 100°C for 20 min. This allows formalin crosslinking to be reversed. The second heating step is performed in a thermomixer at 80°C, with agitation at 750 rpm for 2 h to ensure the highest protein solubilization. After centrifugation at 14000 g at 4°C, extracted proteins were recovered from the supernatant. Protein quantification was then carried out using the Qubit 4 fluorometer (Thermo Fisher Scientific) and protein assay kit (Thermo Fisher Scientific).

### Western blotting

Two polyacrylamide gel formulations (10% and 6% acrylamide) were used to detect proteins of low (GDF9, IHH, and SHH) and high (PTCH1, GLI1, GLI2, and GLI3) molecular weight, respectively. Two different molecular weight markers (ladders) appropriate for proteins with small (PageRuler™ prestained protein ladder, 10–180 kDa, Thermo Fisher Scientific) and large (HiMark™ prestained protein standard, 31–460 kDa, Thermo Fisher Scientific) molecular mass were used. Seven microliters of FFPE proteins extracted from each sample (around 30  $\mu$ g/ml) were mixed with 2.5- $\mu$ l fresh Laemmli sample buffer (100- $\mu$ l  $\beta$ -mercaptoethanol in 900- $\mu$ l buffer) and placed on a heated plate at 95°C for 5 min before loading into the gel wells next to the loaded ladder. Migration of proteins based on size occurs first at 120 V for 10 min and then at 150 V for at least 40 min until the blue marker reaches the bottom limit of the gel. Since proteins need to be accessible for antibody detection, they are transferred from the gel to a polyvinylidene difluoride (PVDF) membrane at 100 V for 1 h. Before incubating with the primary antibody, a blocking step is required to inhibit

**Table 2** Immunostaining patterns of the GDF9-HH-GLI pathway in follicles and stromal cells in fetal ovaries

Protein	Follicle type (n)	Oocytes		Granulosa cells		Stromal cells	
		Nucleus	Cytoplasm	Nucleus	Cytoplasm	Nucleus	Cytoplasm
GDF9	1 (426)	-	+	-	-	-	-
	2 (198)	-	+	-	-	-	-
IHH	1 (879)	-	+	-	++	-	++
	2 (12)	-	+	-	++	-	++
DHH	1 (780)	-	++	-	++	-	++
	2 (11)	-	+	-	++	-	++
SHH	1 (1304)	-	++	-	+ / ++	-	++
	2 (17)	-	++	-	++	-	++
PTCH1	1 (804)	-	+	-	-	-	- / +
	2 (24)	-	+	-	+	-	- / +
GLI1	1 (1051)	- / ++	- / ++	- / ++	- / ++	- / ++	- / ++
	2 (51)	++	++	++	++	++	++
GLI2	1 (117)	- / ++	++	- / ++	- / ++	- / ++	- / ++
	2 (0)	o	o	o	o	o	o
GLI3	1 (623)	- / +	+	+	++	- / +	- / ++
	2 (0)	o	o	o	o	o	o

Staining scored as follows: -, no staining observed; +, moderate staining; ++, strong staining. No type 2 follicles found on the slides

interactions between the membrane and the primary antibody. For this, the membrane is incubated in 5% blocking solution (5-g non-fat dried milk in TBS-T 1× [100-ml TBS + 100-μl 100% Tween 20]) for 1 h at RT. It is then incubated with the primary antibody (overnight at 4°C with gentle agitation) against the protein of interest diluted in 0.5% of the previous blocking solution. After 3 rinses (5 min each) in TBS-T to remove the unbound primary antibody, the membrane is incubated (1 h at RT with gentle agitation) with the secondary antibody (goat anti-mouse Ig [115-035-062, Jackson ImmunoResearch, Pennsylvania, USA] or goat anti-rabbit Ig [111-035-144, Jackson ImmunoResearch, Pennsylvania, USA]) diluted in 0.5% of the blocking solution. The secondary antibody is linked to a peroxidase (HRP) to ensure clear identification of the protein of interest on the membrane, allowing its detection through a chemiluminescent reaction using SuperSignal West Pico PLUS Chemiluminescent Substrate (35477, Thermo Fisher Scientific). This is based on a substrate present in the kit, which recognizes HRP in the secondary antibody and produces light that can be visualized using Fusion software (Vilber Lourmat, Collégien, France).

### RNA extraction and cDNA synthesis

Five human control ovarian tissue samples (age range, 52–79 years; mean age, 63.8) were frozen in Tissue-Tek® O.C.T.™ compound (Sakura, Zoeterwoude, Netherlands) and cut into 5-μm sections with the Thermo Scientific Microm HM560 Cryostat-Series (Thermo Fisher Scientific). Tissue processing

was performed as previously described [22]. Briefly, fragments were placed in lysing matrix Z tubes (MP Biomedicals, Ohio, USA) containing 2-mm yttria-stabilized zirconium beads with 600-μl RLT Plus buffer from the AllPrep DNA/RNA Micro Kit (Qiagen) with 1% β-mercaptoethanol (Sigma-Aldrich, Steinheim, Germany). Samples were lysed by bead beating for two 30-s cycles at 6 m/s in FastPrep lysing matrix Z tubes. A cooling step on ice (40-s cycles) was performed between the two bead beatings. Tubes containing the lysates were then centrifuged for 3 min at 14000 g. Supernatant was collected, and RNA extracted according to the manufacturer's instructions. Isolated RNA concentrations were measured using the Qubit 4 fluorometer and Qubit RNA broad range assay kit (Thermo Fisher Scientific). The QuantiTect whole transcriptome kit (Qiagen) was used to synthesize and amplify cDNA from 20 ng of isolated RNA. Synthesized cDNA concentrations were measured using the Qubit 4 fluorometer and Qubit dsDNA broad range assay kit (Thermo Fisher Scientific).

### Quantitative real-time polymerase chain reaction (qPCR)

mRNA expression of *Gdf9*, *Ihh*, *Gli1*, *Gli2*, and *Gli3* was investigated by quantitative real-time PCR using TaqMan probes for *Gdf9* (Hs03986126-s1), *Ihh* (Hs00745531-s1), *Gli1* (Hs00171790-m1), *Gli2* (Hs01119974-m1), and *Gli3* (Hs00609233-m1). *Rplp0* (Hs99999902-m1) and *B2M* (Hs00187842\_m1) served as housekeeping genes. cDNA from 10 reproductive-age human ovaries was used as positive

**Table 3** Immunostaining patterns of the GDF9-HH-GLI pathway in follicles and stromal cells in prepubertal ovaries

Protein	Follicle type ( <i>n</i> )	Oocytes		Granulosa cells		Theca cells		Stromal cells	
		Nucleus	Cytoplasm	Nucleus	Cytoplasm	Nucleus	Cytoplasm	Nucleus	Cytoplasm
GDF9	1 (1360)	-	+/++	-	-	o	o	-	-
	2 (50)	-	+/++	-	-	o	o	-	-
	3 (3)	-	+	-	-	o	o	-	-
	4 (0)	oo	oo	oo	oo	oo	oo	-	-
IHH	1 (1477)	-	+/++	-	++	o	o	-	+
	2 (102)	-	+	-	++	o	o	-	-
	3 (3)	-	++	-	++	o	o	-	-
	4 (0)	oo	oo	oo	oo	oo	oo	-	-
DHH	1 (1360)	-	+/++	-	++	o	o	-	++
	2 (50)	-	+/++	-	++	o	o	-	-
	3 (3)	-	+	-	++	o	o	-	-
	4 (0)	oo	oo	oo	oo	oo	oo	-	-
SHH	1 (3962)	-	++	-	++	o	o	-	-/+
	2 (34)	-	++	-	++	o	o	-	-
	3 (2)	-	++	-	++	o	o	-	-
	4 (2)	-	+	-	+	-	-	-	-
PTCH1	1 (2096)	-	+	-	+	o	o	-	-/+
	2 (39)	-	+	-	+	o	o	-	-
	3 (1)	-	+	-	+	o	o	-	-
	4 (0)	oo	oo	oo	oo	oo	oo	-	-
GLI1	1 (2114)	-/+	-/+	-/+	-/+	o	o	-/+	-/+
	2 (77)	-/+	-/+	-/+	-/+	o	o	-/+	-/+
	3 (2)	-	+	++	+	-	-	-	-
	4 (2)	-	+	++	+	-	-	-	-
GLI2	1 (2957)	-/+	++	++	++	o	o	-/+	-/+
	2 (35)	-/+	++	++	++	o	o	-/+	-/+
	3 (4)	-/+	+/++	-/+	-/+	o	o	-/+	-/+
	4 (3)	++	++	++	++	-	-	-	-
GLI3	1 (2396)	-/+	+	-/+	+	o	o	++	++
	2(79)	-/+	+	-/+	+	o	o	++	++
	3 (4)	+	+	+	+	o	o	++	++
	4 (1)	-	+	++	+	-	-	-	-

Staining scored as follows: -, no staining observed; +, moderate staining; ++, strong staining

Type 1 to 3 follicles not yet surrounded by a theca layer

No type 4 follicles found on the slides

controls for Gli1 (data not shown), and cDNA from two individual hepatocyte samples were used as the control for Gli1, Gli2, and Gli3 (data not shown). A total of 1-µl primer; 7-µl pyrogen, DNase, and RNase-free diethyl pyrocarbonate (DEPC) water (Invitrogen, Thermo Fisher Scientific); 10-µl TaqMan Gene Expression Master Mix (Thermo Fisher Scientific); and 2-µl cDNA (50 ng/µl) was added to each well. Target genes were analyzed in duplicate for each sample. Standard cycling conditions were applied as recommended by the manufacturer. Thermal cycling and fluorescence detection were performed using the StepOnePlus real-time PCR system (Applied Biosystems, California, USA).

## Results

### Immunohistochemistry

Although no statistical analyses were performed, ovaries from 14- and 33-week-old fetuses were quite different in morphology from each other. In the youngest fetal ovaries (14 weeks), the cell population was a mixture of stromal cells and oogonia (Fig. 1a). At around 17 weeks, some oocytes were observed in addition to oogonia in fetal ovaries (Fig. 1b). From approximately week 22 onward, primordial follicles are known to emerge, and primary oocytes are surrounded by one layer of

**Table 4** Immunostaining patterns of the GDF9-HH-GLI pathway in follicles and stromal cells in reproductive-age ovaries

Protein	Follicle type (n)	Oocyte		Granulosa cells		Theca cells		Stromal cells	
		Nucleus	Cytoplasm	Nucleus	Cytoplasm	Nucleus	Cytoplasm	Nucleus	Cytoplasm
GDF9	1 (170)	-	+	-	-	°	°	-	+ / ++
	2 (89)	-	+	-	-	°	°		
	3 (4)	-	+	-	-	°	°		
	4 (3)	-	+	-	+	-	+		
	5 (0)	°°	°°	°°	°°	°°	°°		
	6 (11)	-	-	-	+	-	+		
IHH	1 (69)	-	+	-	-	°	°	-	+ / ++
	2 (55)	-	+	-	++	°	°		
	3 (7)	-	+	-	+	°	°		
	4 (1)	-	-	-	++	-	+		
	5 (0)	°°	°°	°°	°°	°°	°°		
	6 (14)	-	-	-	- / +	-	++		
DHH	1 (143)	-	+	-	-	°	°	-	++
	2 (75)	-	+	-	++	°	°		
	3 (13)	-	+	-	++	°	°		
	4 (7)	-	+	-	++	-	+		
	5 (0)	°°	°°	°°	°°	°°	°°		
	6 (18)	-	-	-	++	-	+		
SHH	1 (89)	-	++	-	++	°	°	-	++
	2 (55)	-	++	-	++	°	°		
	3 (10)	-	+	-	++	°	°		
	4 (3)	-	+	-	+	-	++		
	5 (0)	°°	°°	°°	°°	°°	°°		
	6 (7)	-	-	-	+ / ++	-	++		
PTCH1	1 (94)	-	++	-	+	°	°	-	+
	2 (48)	-	+	-	+	°	°		
	3 (8)	-	+	-	++	°	°		
	4 (0)	°°	°°	°°	°°	°°	°°		
	5 (2)	-	+	-	- / +	-	++		
	6 (9)	-	-	-	+	-	++		
GLI1	1 (85)	++	+	+	+	°	°	- / ++	- / ++
	2 (102)	++	+	++	++	°	°		
	3 (20)	++	+	++	++	°	°		
	4 (4)	++	+	++	+	++	++		
	5 (3)	+	+	++	+	++	++		
	6 (13)	-	-	++	++	++	++		
GLI2	1 (92)	- / ++	++	++	++	°	°	- / ++	- / +
	2 (104)	- / ++	+	- / + / ++	- / + / ++	°	°		
	3 (10)	++	+	++	+	°	°		
	4 (6)	++	+	++	+	++	-		
	5 (0)	°°	°°	°°	°°	°°	°°		
	6 (12)	-	-	++	+	++	+		
GLI3	1 (101)	-	+	++	++	°	°	- / ++	- / ++
	2 (92)	-	+ / ++	+	+	°	°		
	3 (9)	+	+ / ++	+	+	°	°		
	4 (3)	+	+	++	+	-	-		
	5 (2)	-	-	+ / ++	+	+	-		
	6 (7)	-	-	+ / ++	- / +	- / +	-		

Staining scored as follows: -, no staining observed; +, moderate staining; ++, strong staining

°Type 1 to 3 follicles not yet surrounded by a theca layer

°°No follicles found on the slides

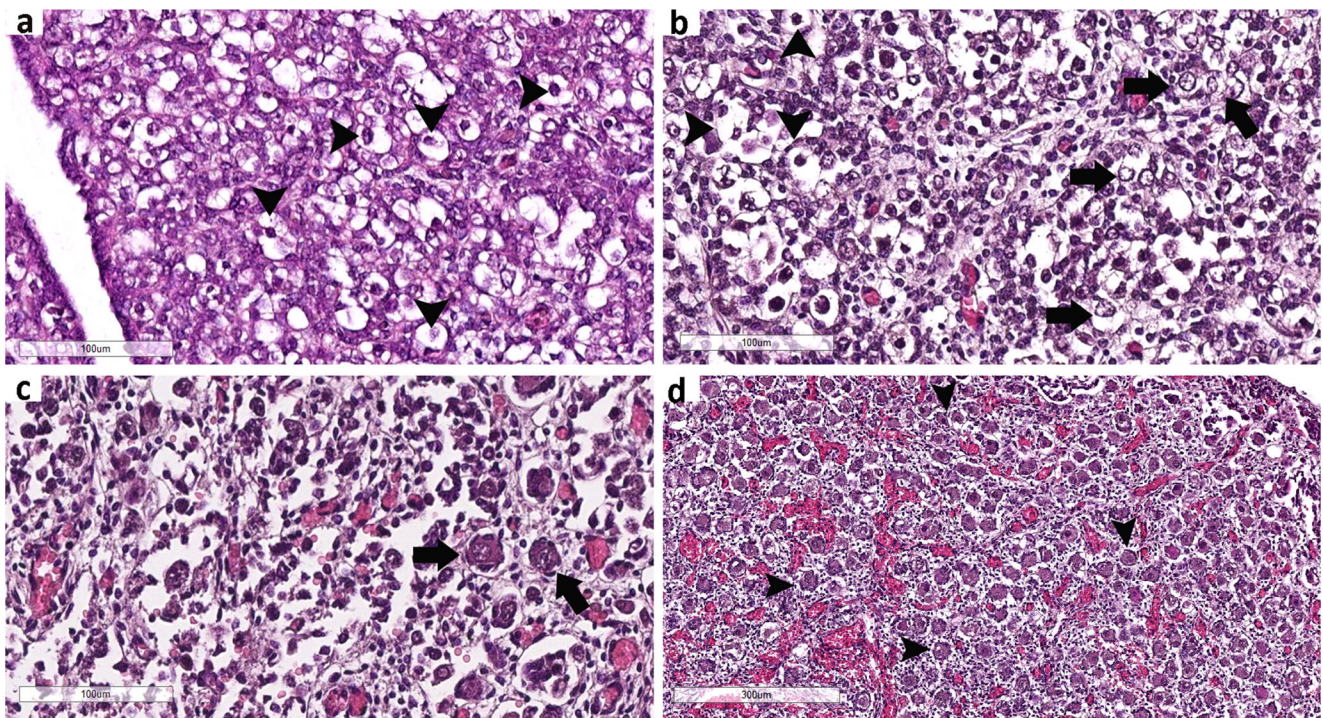


**Fig. 1** Histological sections of fetal ovaries at different time points of gestation. At around 14 weeks, oogonia (arrowhead) are visible (a). At around 17 weeks, oocytes (arrow) can be observed (b). At around 22

weeks, type 1 follicles (arrow) are found in the ovaries (c). At around 33 weeks (d), the ovary contains many type 1 follicles (arrow). Scale bar: 100 μm (a, b, and c), 300 μm (d)

follicular cells, which will later form granulosa cells (Fig. 1c). Fetal ovaries at 33 weeks (Fig. 1d) contain the pool of primordial follicles that a girl will be born with. In our tissue samples from newborns to 2-year-old girls, the number of primordial follicles was still high, and up to 150 follicles were counted in each ovarian section (Fig. 2a). By the age of 6 years, the ovarian reserve had already declined (Fig. 2b). It is interesting to note that in the prepubertal group, additional follicle stages (type 2, type 3, and type 4) appeared in the stroma (Fig. 2c).

Descriptive immunohistochemical analysis of follicles in fetal ovaries revealed expression of GDF9, IHH, DHH, SHH, PTCH1, GLI1, GLI2, and GLI3 in the oocyte cytoplasm (Table 2; Figs. 3, 4, 5, 6, 7, 8, 9, and 10). All members of the HH family were also strongly expressed in the cytoplasm of follicular/granulosa cells (Figs. 3, 4, 5, 6, 7, 8, 9, 10). Stromal cells were positive for IHH, DHH, SHH, and PTCH1 only in their cytoplasm and for GLI1, GLI2, and GLI3 in the cytoplasm and sometimes in the nucleus (Table 2; Figs. 3, 4, 5, 6, 7, 8, 9, 10).

In ovaries from newborn to 6-year-old girls, GDF9 staining was specific to the oocyte and some stromal cells cytoplasm (Table 3; Fig. 3). HH ligands (IHH, DHH, and SHH) were expressed in oocytes and the granulosa cell cytoplasm in types 1 to 3 follicles, showing moderate to strong staining (Table 3; Figs. 4, 5, 6). As in fetal ovaries, there was weak staining for PTCH1 receptor in the cytoplasm of oocytes and granulosa cells from type 1 to 3 follicles (Table 3; Fig. 7). It is important

to note that GDF9, IHH, DHH, and PTCH1 expressions were not possible to assess in type 4 follicles, as they were not detected in sections used for protein staining. Transcription factors GLI1, GLI2, and GLI3 showed positive nuclear and/or cytosolic staining in oocytes and granulosa cells in type 1 to 4 follicles (Table 3; Figs. 8, 9, 10). Only type 4 follicles contained a layer of theca cells, which did not stain any protein involved in the studied pathway. Stromal cells exhibited immunostaining for all markers except GDF9, but their nuclei expressed only GLI1, GLI2, and GLI3 (Table 3; Figs. 8, 9, 10).

In reproductive-age subjects, follicles continue their growth up to the final stages of development. Unlike prepubertal ovaries, where a great number of primordial follicles were observed, in the reproductive-age group, this follicle population appeared less abundant. On the other hand, in the latter group, type 5 and 6 follicles were identified. At this stage of development, the cortex and medulla can be easily distinguished from each other, and the majority of follicles are located in the cortex. IHC in reproductive-age ovaries showed cytoplasmic expression of GDF9 in oocytes of type 1 to 4 follicles and granulosa and theca cells of type 5 and 6 follicles, at the same moderate intensity (Table 4; Figure 3). Staining for HH ligands was observed in the cytoplasm of both oocytes and granulosa cells for type 1 to 6 follicles (Table 4; Figs. 4, 5, 6). Type 5 follicles were not detected on slides used for GDF9, IHH, DHH, and SHH staining, but PTCH1 expression was

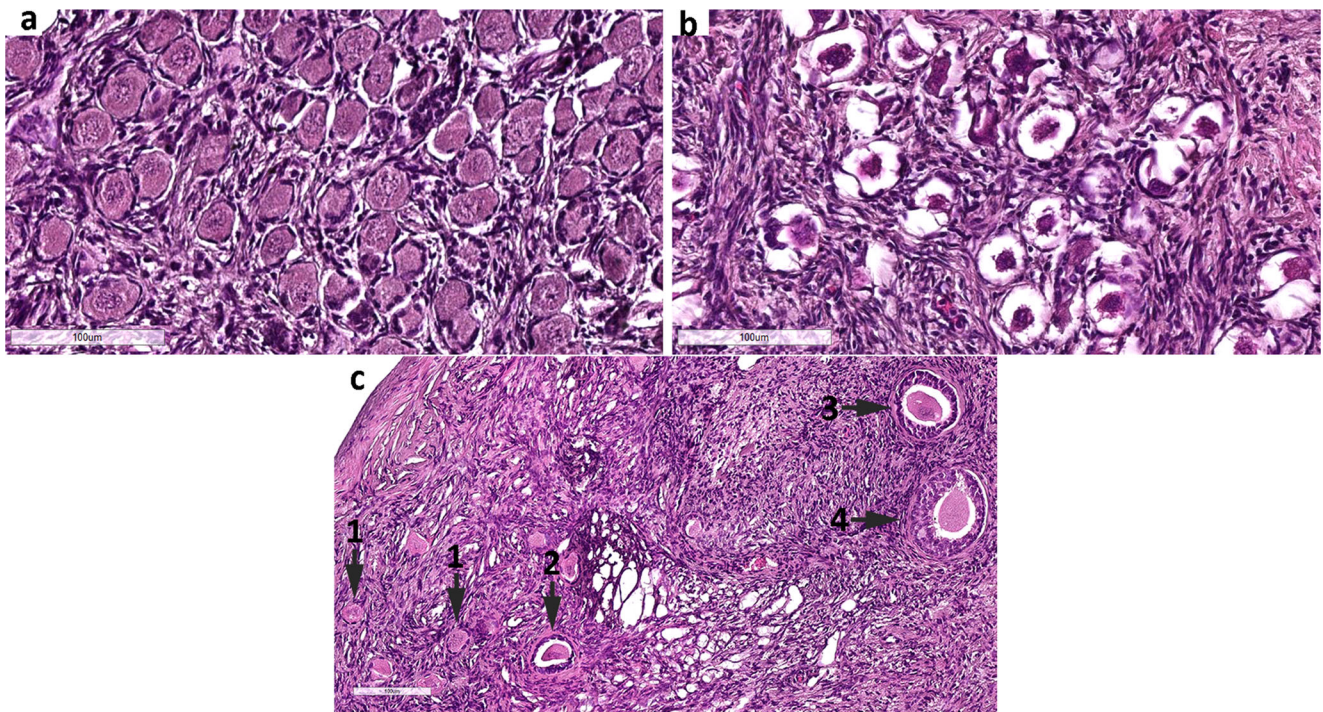


**Fig. 2** Histological sections of prepubertal ovaries at around the time of birth age 6. Abundant population of type 1 follicles in a newborn girl (a). Decrease in the number of type 1 follicles in the ovary of a 6-year-old girl

(b). Presence of types 2, 3, and 4 follicles in addition to type 1 (shown by arrow) in the ovary of a 6-year-old girl (c). Scale bar: 100  $\mu$ m

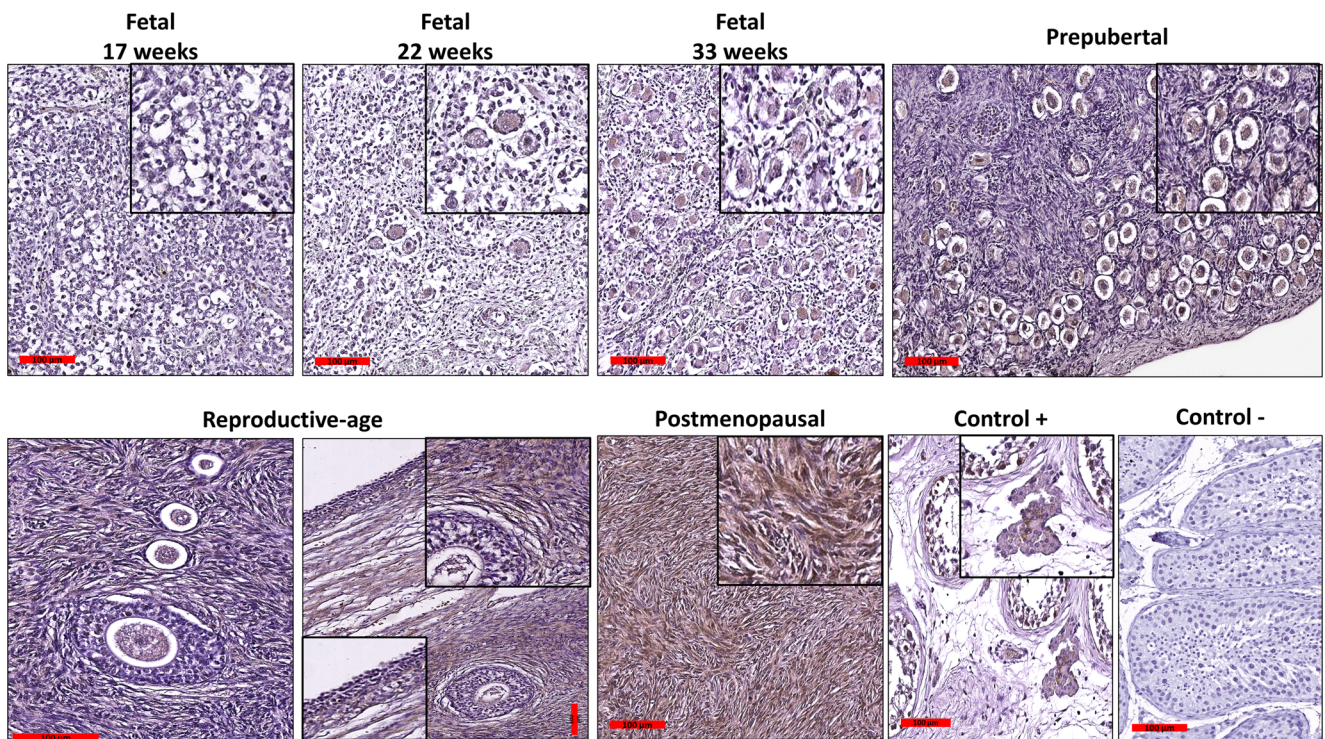


**Fig. 3** Immunohistochemical staining of GDF9 in fetal, prepubertal, reproductive-age, and postmenopausal ovaries. No staining for GDF9 in a 17-week-old fetal ovary; GDF9 cytoplasmic staining in oocytes from type 1 follicles in 22- and 33-week-old fetal ovaries; GDF9 cytoplasmic staining in oocytes from type 1 follicles and stromal cells in prepubertal

ovaries; GDF9 cytoplasmic staining in oocytes from types 1, 2, 3, and 4 follicles and stromal cells in reproductive-age ovaries and the theca interna and externa of type 5 and 6 follicles; GDF9 cytoplasmic expression in postmenopausal ovarian stromal cells; testes as positive and negative controls for GDF-9. Scale bar: 100  $\mu$ m



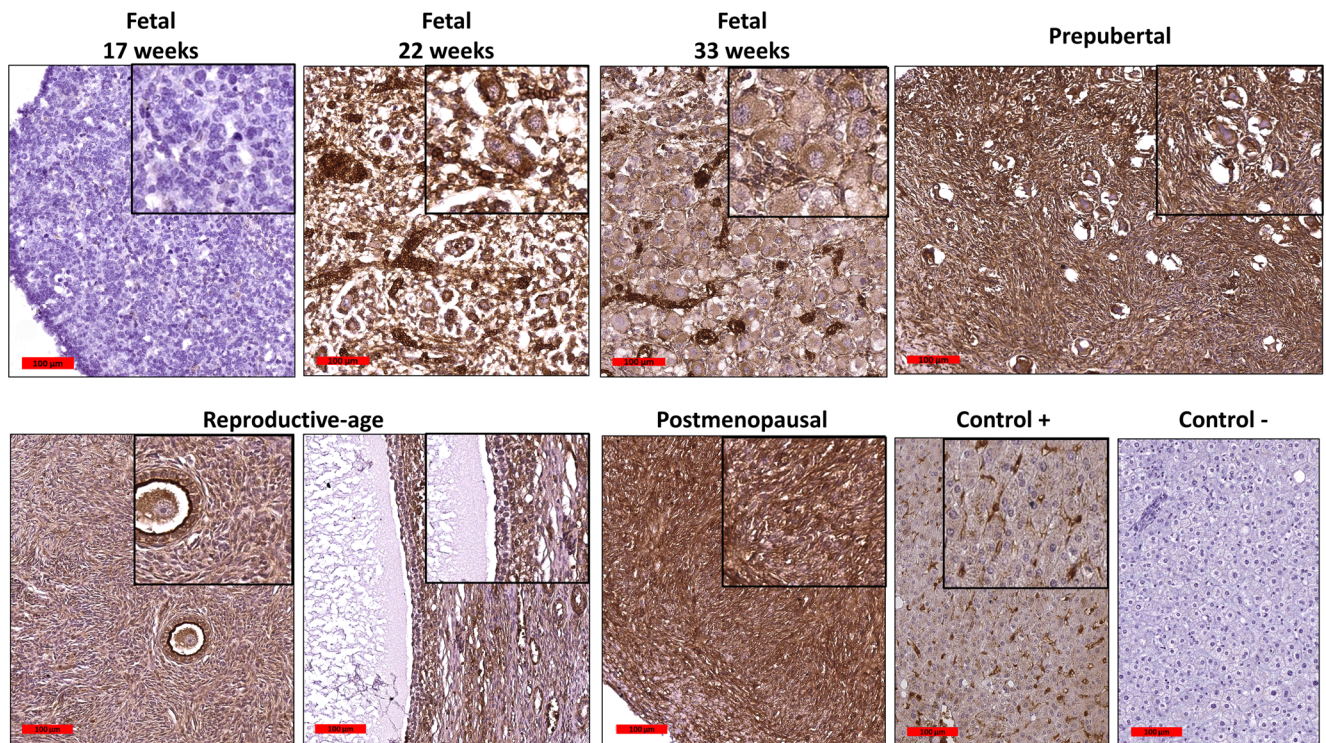


**Fig. 4** Immunohistochemical staining of IHH in fetal, prepubertal, reproductive-age, and postmenopausal ovaries. No staining for IHH in the ovary of a 17-week-old fetus; IHH cytoplasmic staining of oocytes, granulosa, and stromal cells in 22- and 33-week-old fetuses and prepubertal ovaries; IHH cytoplasmic staining in oocytes, granulosa, theca interna and externa, and stromal cells in reproductive-age ovaries; IHH cytoplasmic staining in postmenopausal ovarian stromal cells; liver as positive and negative controls for IHH. Scale bar: 100  $\mu$ m

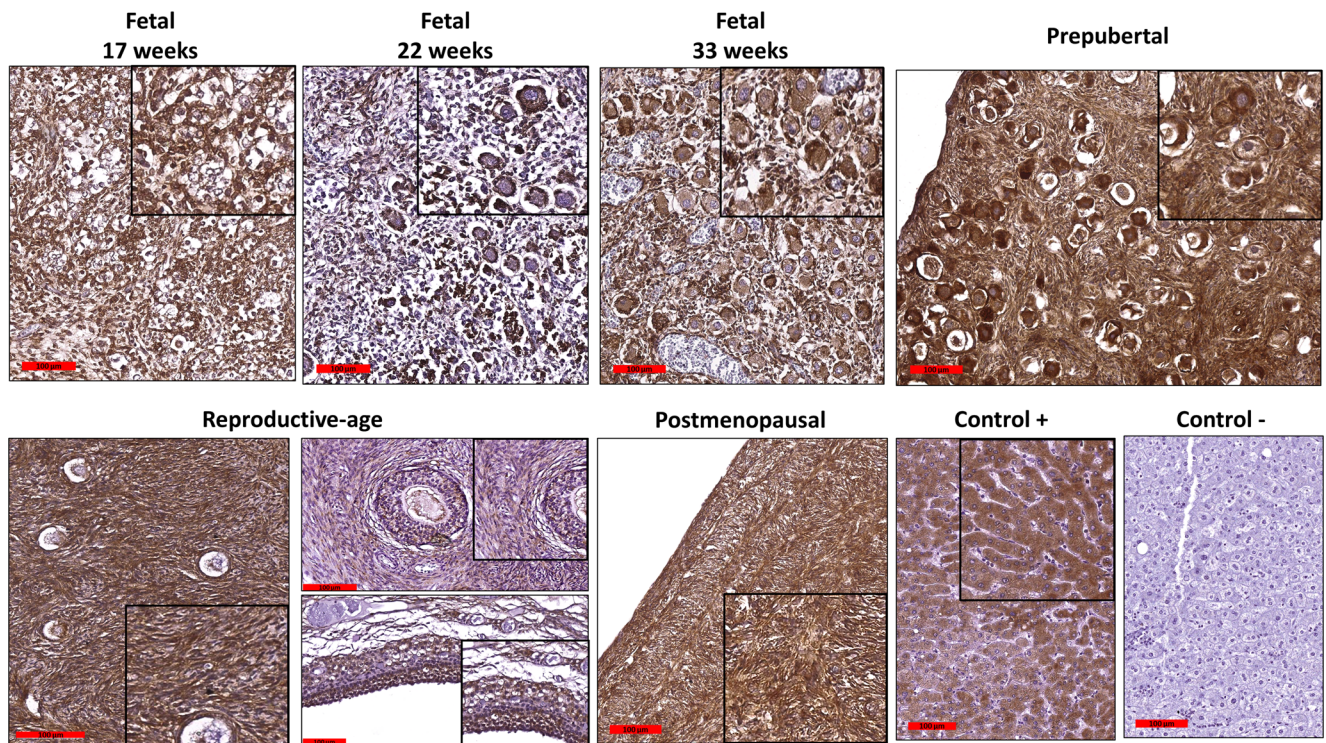


**Fig. 5** Immunohistochemical staining of DHH in fetal, prepubertal, reproductive-age, and postmenopausal ovaries. DHH cytoplasmic staining of ovarian cells and oocyte in fetal and prepubertal ovaries; DHH cytoplasmic staining of oocytes, granulosa, theca interna and externa, and stromal cells in reproductive-age ovaries; DHH cytoplasmic staining in postmenopausal ovarian stromal cells; liver as positive and negative controls for DHH. Scale bar: 100  $\mu$ m

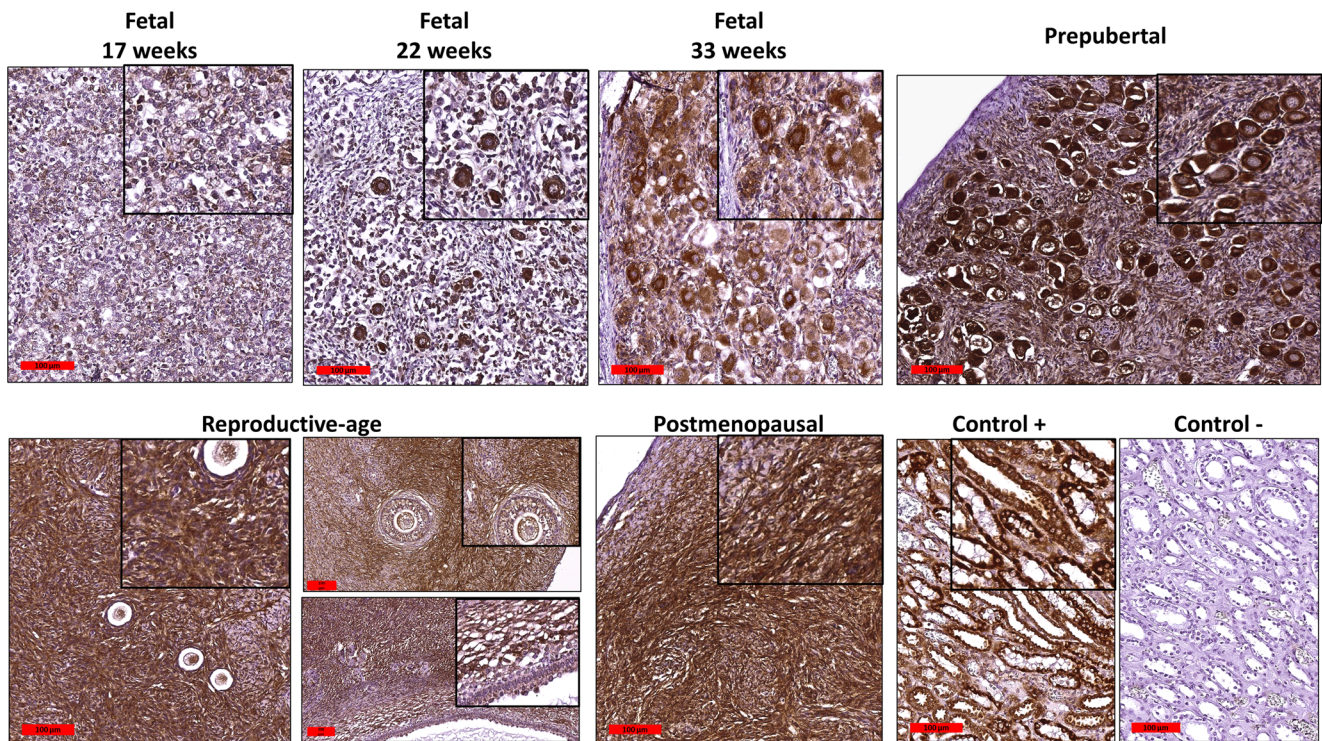


**Fig. 6** Immunohistochemical staining of SHH in fetal, prepubertal, reproductive-age, and postmenopausal ovaries. SHH cytoplasmic staining of stromal cells and oocytes in fetal and prepubertal ovaries; SHH cytoplasmic staining of oocytes, granulosa, theca interna and

externa, and stromal cells in reproductive-age ovaries; SHH cytoplasmic staining in postmenopausal ovarian stromal cells; kidney as positive and negative controls for SHH. Scale bar: 100 μm

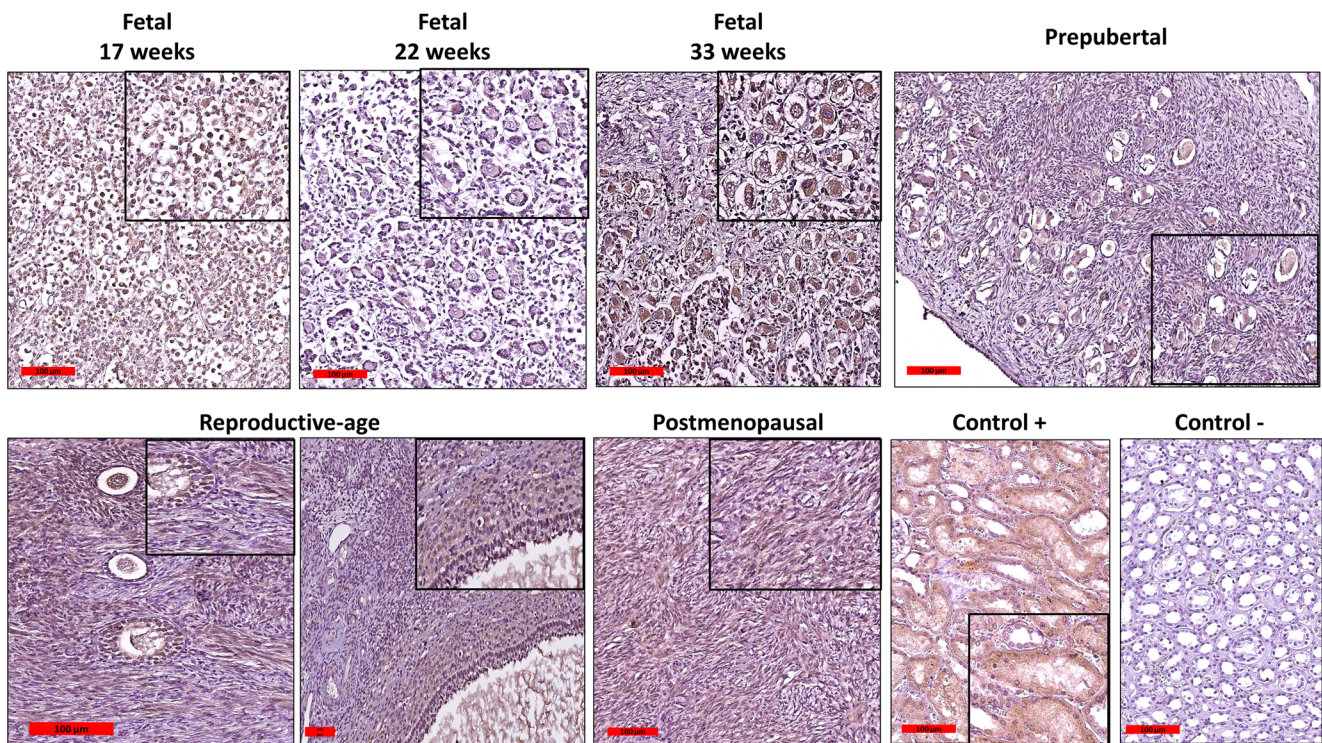


**Fig. 7** Immunohistochemical staining of PTCH1 in fetal, prepubertal, reproductive-age, and postmenopausal ovaries. PTCH1 cytoplasmic staining of oogonia and ovarian cells of 17-week-old fetal ovary; PTCH1 cytoplasmic staining of oocytes and some ovarian cells in 22- and 33-week-old fetal ovaries; PTCH1 cytoplasmic staining in oocytes

and some stromal cells in prepubertal ovaries; PTCH1 cytoplasmic staining of oocyte, granulosa cells, theca interna and externa, and stromal cells in reproductive-age ovaries; PTCH1 cytoplasmic staining in postmenopausal ovarian stromal cells; kidney as positive and negative controls for PTCH1. Scale bar: 100 μm

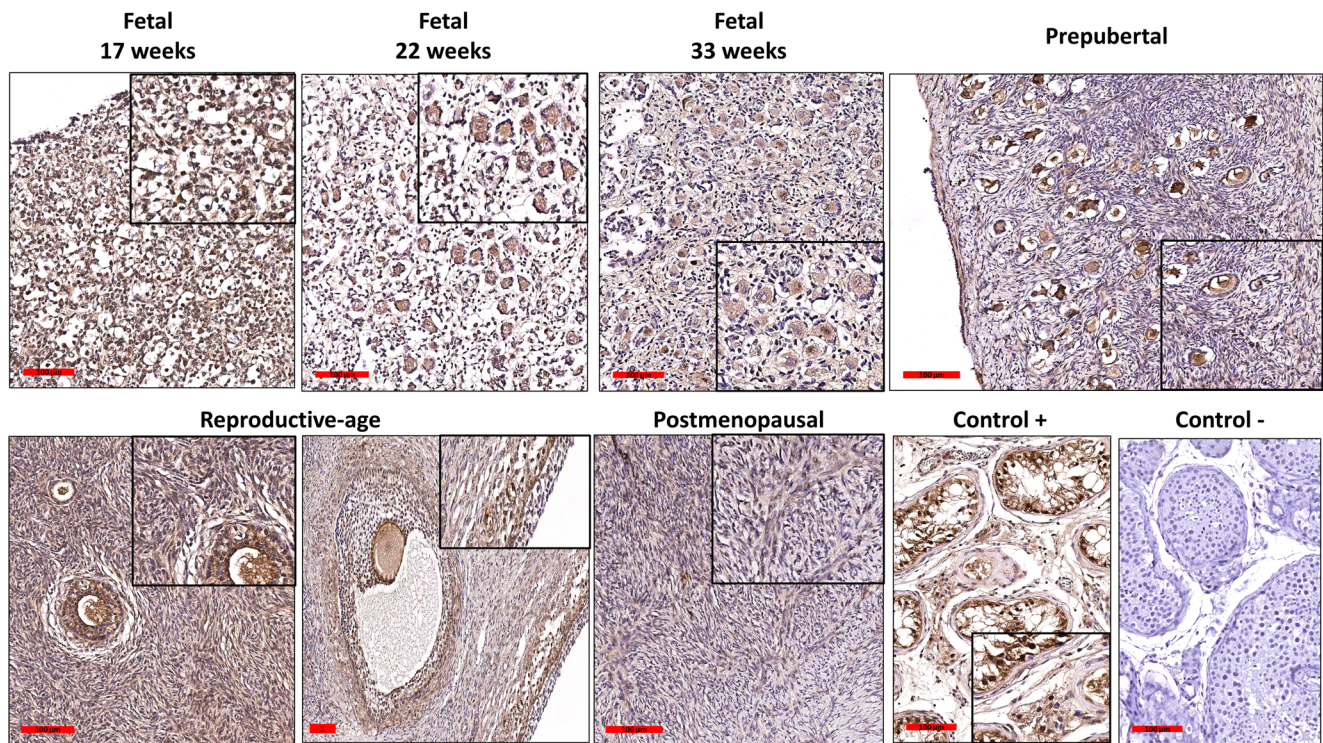


**Fig. 8** Immunohistochemical staining of GLI1 in fetal, prepubertal, reproductive-age, and postmenopausal ovaries. GLI1 cytoplasmic and nuclear staining of oogonia and ovarian cells of 17-week-old fetal ovary; GLI1 cytoplasmic and nuclear staining of oocytes in 22- and 33-week-old fetal ovaries; GLI1 cytoplasmic and nuclear staining of oocytes and cytoplasmic staining of ovarian stromal cells in prepubertal ovaries;

GLI1 cytoplasmic and nuclear staining of oocytes, theca interna and theca externa, and cytoplasmic staining of granulosa cells and ovarian stromal cells in reproductive-age ovaries; GLI1 weak cytoplasmic staining in some postmenopausal ovarian stromal cells; testes as positive and negative controls for GLI1. Scale bar: 100  $\mu$ m

seen in the oocyte cytoplasm of type 1 to 5 follicles. On the other hand, PTCH1 displayed immunostaining in the cytoplasm of granulosa cells in type 1 to 6 follicles (Table 4; Fig. 7). Theca cells in type 5 and type 6 follicles showed moderate PTCH1 expression in their cytoplasm (Table 4; Fig. 7), but those in type 4 and 6 follicles showed moderate to strong cytoplasmic staining for HH ligands (Table 4; Figs. 4, 5, 6). GLI1, GLI2, and GLI3 were expressed in oocytes, granulosa, and theca cells at most stages of follicle development (Table 4; Figs. 8, 9, 10). However, GLI3 was less expressed than other isoforms. Unexpectedly, stromal cells exhibited moderate to strong expression of GDF9 in their cytoplasm, which showed immunostaining for HH ligands and PTCH1 too. All studied GLI proteins were also stained at varying intensities in the cytoplasm and/or nucleus of stromal cells (Table 4; Figs. 3, 4, 5, 6, 7, 8, 9, 10).

Since there are no follicles in postmenopausal ovaries, we focused our analysis on the stromal cell population. In the postmenopausal group, we investigated the entire stroma, as in all other groups. Like reproductive-age ovaries, stromal cells from their menopausal counterparts showed different intensities of staining for GDF9 (Table 5; Fig. 3). GDF9 expression was localized in the cytoplasm of stromal cells, and its intensity differed from one patient to another (Table 5). IHH,

DHH, and SHH were also detected in the same cell compartment (Table 5). Weak cytosolic PTCH1 expression was observed, and GLI1, GLI2, and GLI3 showed different staining intensities in the nucleus and cytoplasm of stromal cells (Table 5; Figs. 3, 4, 5, 6, 7, 8, 9, 10).

### Western blot

In order to confirm our findings, we performed Western blotting on the same proteins extracted from the same paraffin blocks previously used in IHC analyses. It is, however, important to stress that we encountered some complications while implementing this technique. Since ovarian tissue from prepubertal girls was encapsulated in agarose prior to paraffin embedding and this procedure affects protein extraction, we had to exclude this group from our Western blot study.

Results were compared with datasheets for commercial antibodies, and positive tissue controls were the same as those used for IHC. For all proteins except DHH, whose antibody was not compatible, Western blotting was carried out on lysates of fetal, prepubertal, reproductive-age, and postmenopausal ovarian tissue samples, as well as positive controls (Fig. 11).

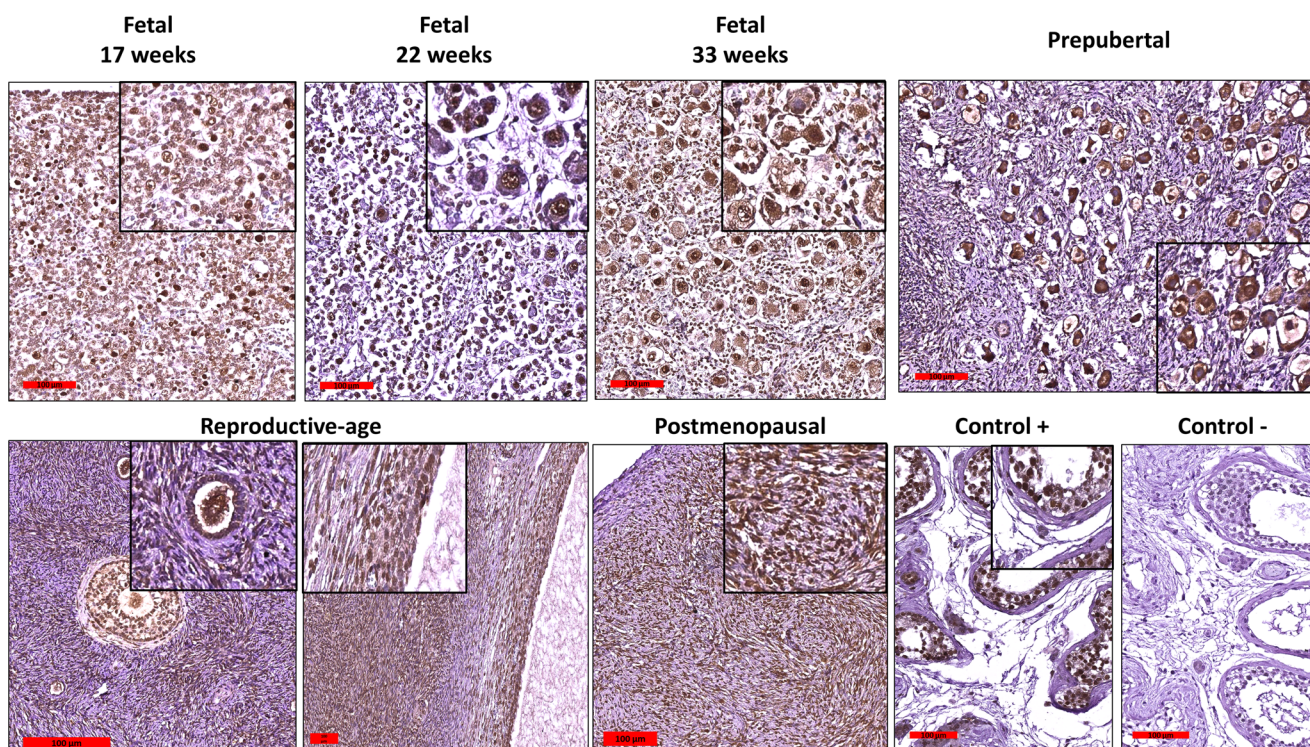


**Fig. 9** Immunohistochemical staining of GLI2 in fetal, prepubertal, reproductive-age, and postmenopausal ovaries. GLI2 cytoplasmic and nuclear staining of oocytes, ovarian, and granulosa cells in fetal ovaries; GLI2 cytoplasmic staining of oocytes and granulosa cells in prepubertal ovaries; GLI2 cytoplasmic and nuclear staining of oocytes, granulosa

cells, theca interna and externa, and ovarian stromal cells of reproductive-age ovaries; GLI2 cytoplasmic and nuclear staining of postmenopausal ovarian stromal cells; testes as positive and negative controls for GLI2. Scale bar: 100  $\mu$ m

## Quantitative real-time PCR

To confirm our IHC and Western blot findings in key proteins in postmenopausal ovaries, we performed quantitative real-time PCR to assess the presence of mRNA for *Gdf9*, *Ihh*, *Gli1*, *Gli2*, and *Gli3* in postmenopausal ovarian tissue, despite the lack of a follicle population. Our results revealed the presence of mRNA for *Gdf9* (mean Ct value=22.8), *Ihh* (mean Ct value=26.2), and *Gli3* (mean Ct value=31.9) in stromal cells from all five postmenopausal ovaries, *Gli2* (Ct value=35.4) in one of the five postmenopausal ovaries, but no mRNA transcripts for *Gli1* in any of the samples (Fig. 11).

## Discussion

While theca cells play a pivotal role in follicle development, steroid production, and ovulation, there is not much information on their origin, recruitment, and differentiation in human ovaries. Although there are some studies indicating that it occurs under the influence of different factors expressed by oocytes and granulosa cells of growing follicles (reviewed by [23]), only a few hypothesize on the origin of these cells. It has been postulated from studies directly on isolated mouse ovarian tissue [9] or in vitro cultured [24] that stromal cells

surrounding follicles are those recruited for further differentiation (reviewed by [25]). More recently, in vitro studies in large animal models suggest that all stromal cells, not only those close to follicles, can differentiate into theca cells [26, 27]. However, we have demonstrated that while most human stromal cells can differentiate into steroidogenic cells in vitro, only a small proportion of them can actually become theca- and luteal-like cells [28]. This has led us to speculate that, just like in mouse ovaries [3, 5], there is a population of precursor theca cells in their human counterparts. In pursuit of this theory, we assessed the GDF9-HH-GLI pathway in human fetal, prepubertal, reproductive-age, and postmenopausal ovaries, as this pathway has been shown to be fundamental to recruiting precursor theca cells expressing *Gli1* in neonatal mice ovaries as a marker [3]. Our results revealed that this pathway originates from primordial follicles during the fetal period of life, and not from the primary stage after birth, as in mouse ovaries [10, 29, 30]. Based on our findings, GLI1, GLI2, and GLI3 proteins do not appear to be specific markers for precursor theca cells in human ovaries. First, they are not confined to a specific population of cells, as they are expressed in oocytes and granulosa cells as well as the stroma and not limited to precursor theca cells in ovarian stroma and differentiated steroidogenic theca cells, as in mice. Furthermore, expression of GLI1, 2, and 3 is not limited to a specific ovary

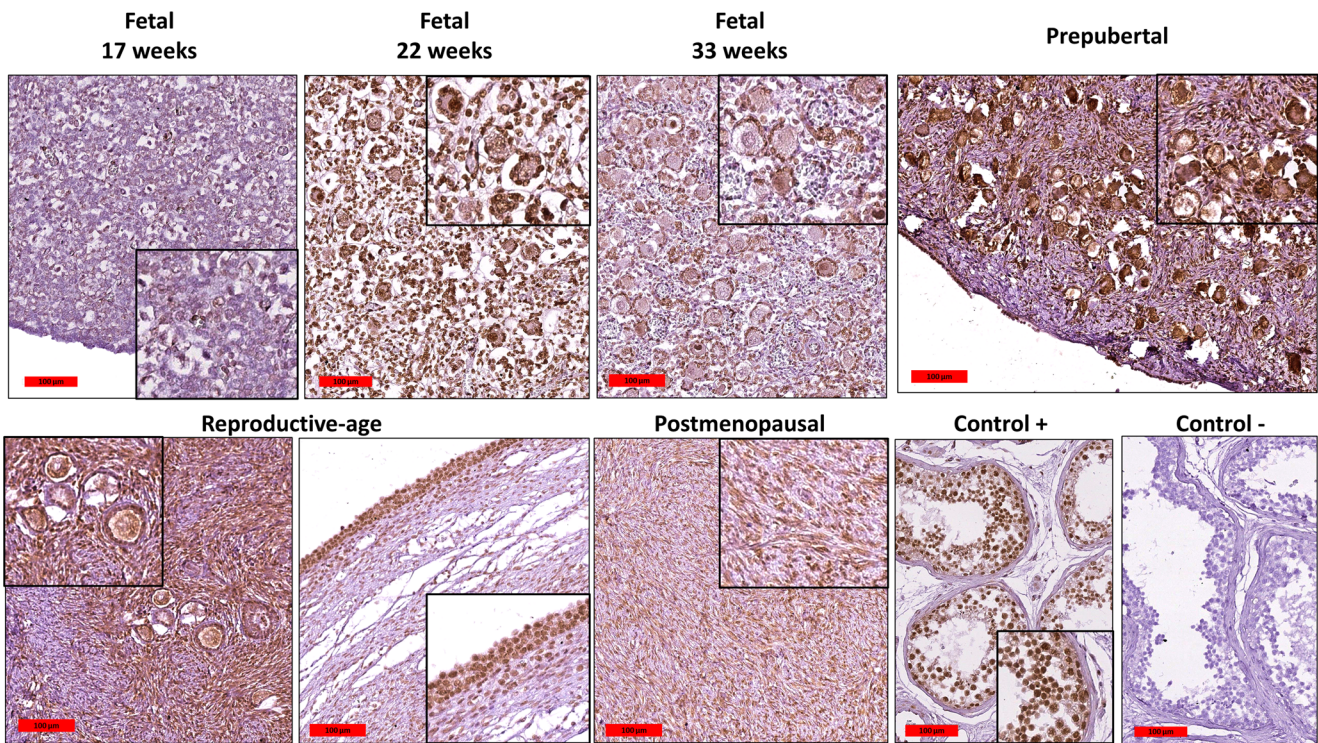


**Fig. 10** Immunohistochemical staining of GLI3 in fetal, prepubertal, reproductive-age, and postmenopausal ovaries. GLI3 cytoplasmic staining of some ovarian cells in 17-week-old fetal ovary; GLI3 nuclear and cytoplasmic staining of oocytes and almost all the ovarian cells in 22-week-old fetal ovaries; GLI3 cytoplasmic and nuclear staining of oocytes, granulosa cells, and most of the ovarian cells in 33-week-old fetal and

prepubertal ovaries; GLI3 cytoplasmic staining of oocytes and cytoplasmic and nuclear staining of granulosa and stromal cells and nuclear staining of theca interna and externa of reproductive-age ovaries; GLI3 cytoplasmic and nuclear staining of postmenopausal ovarian stromal cells; testes as positive and negative controls for GLI3. Scale bar: 100 μm

age, as these proteins are expressed in 17-week-old fetal ovaries as long as the ovary continues to grow and follicles start to appear and develop. Finally, stromal cells from postmenopausal ovaries go on expressing GLI proteins, despite the absence of follicles.

A study on frozen ovarian tissue in mice indicated that the HH and PTCH1 response system might also function in an

autocrine manner in granulosa cells [21]. Moreover, the GDF9-HH-GLI pathway may differ between mammals. For instance, Spicer et al. [31] speculated that differences might exist in terms of hormonal regulation of the HH system between monotocous (cattle) and polytocous (rodents) species. In mammals, HH signaling is a key factor in communication between cellular compartments (gonads, Sertoli cells in testes and granulosa cells in ovaries) involved in gametogenesis and steroidogenesis [9, 11].

While our findings indicate that GLI proteins are not specific markers to identify precursor theca cells in human ovaries, based on GDF9, IHH, DHH, SHH, PTCH1, GLI1, GLI2, and GLI3 expression patterns, we can postulate that the GDF9-HH-GLI pathway may well play a different role in human ovaries. Mutations in the *Gdf9* gene in human and sheep ovaries and various knockout and over-expressed mouse models indicate that GDF9 is crucial to regulating and promoting follicle growth and oocyte development by predominantly acting on supporting granulosa cells via paracrine signaling [32]. Like Sun et al. [33], by using IHC, we also observed GDF9 expression in human ovarian oocytes. Interestingly, our IHC results from prepubertal, reproductive-age, and postmenopausal ovaries showed GDF9 expression in the cytoplasm of stromal cells. Nevertheless, we

**Table 5** Localization and staining intensity patterns of GDF9, IHH, DHH, SHH, PTCH1, GLI1, GLI2, and GLI3 in stromal cells in postmenopausal ovaries

Protein	Stromal cells	
	Nucleus	Cytoplasm
GDF-9	-	-/+ / ++
IHH	-	++
DHH	-	++
SHH	-	++
PTCH1	-	+
GLI1	-	-/+
GLI2	++	-/+
GLI3	-/+	-/+

Staining scored as follows: -, no staining observed; +, moderate staining; ++, strong staining

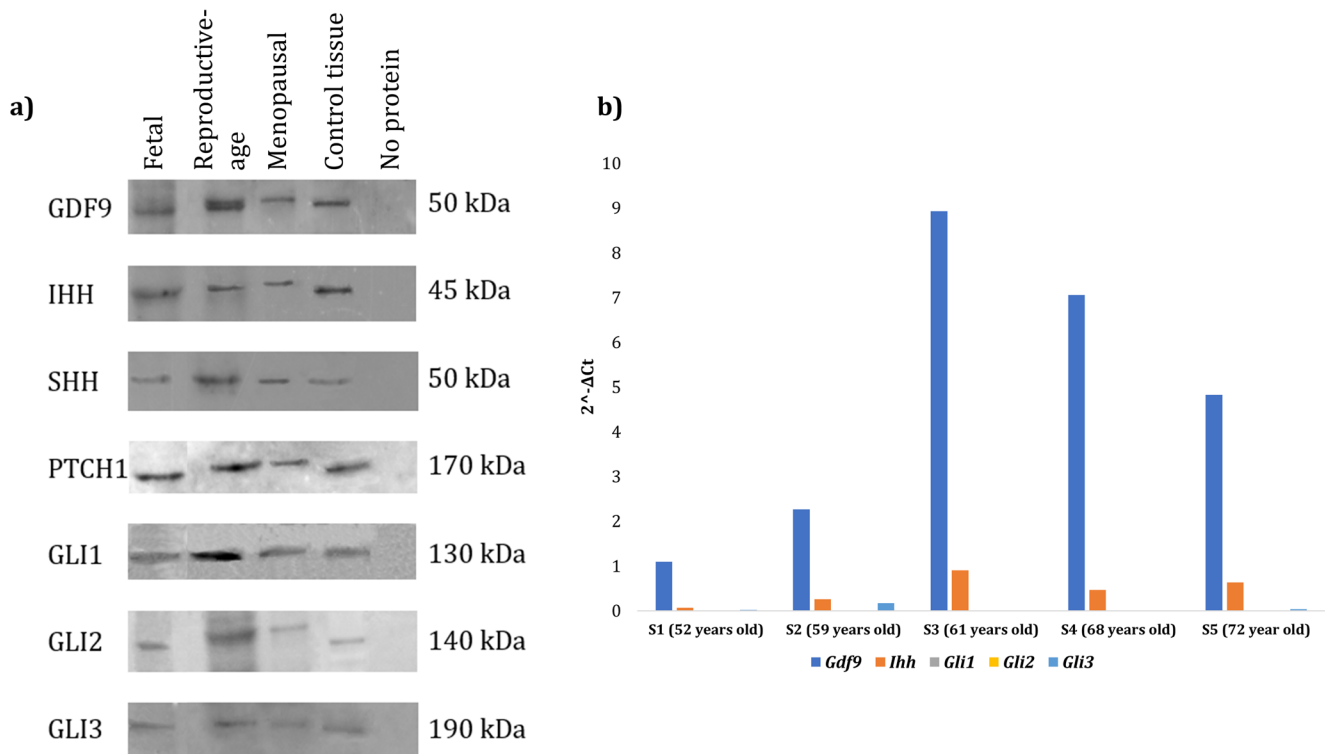


**Fig. 11** Western blot and Ct values from qPCR analysis. Western blotting of the same antibodies as used for immunohistochemistry (a). Ct values were obtained from qPCR for *Gdf9*, *Ihh*, *Gli1*, *Gli2*, and *Gli3* in stromal cells of postmenopausal ovaries.

performed qPCR analysis on samples of postmenopausal ovaries (52–79 years of age), which confirmed the presence of *Gdf9* mRNA in this cell population. To the best of our knowledge, there are no studies explaining this *GDF9* mRNA and protein expression, which is typically associated with folliculogenesis in human ovarian stroma. However, our findings may explain Riepsamen et al.'s [34] observations on the elevated GDF9 serum levels in some postmenopausal women. It would be therefore necessary to perform an in-depth investigation to understand which other origin and roles GDF9 may have in the ovary.

Amino acid sequences of IHH, DHH, and SHH are highly similar. All three HH family members can evoke similar mechanistic responses through the PTCH1 receptor in in vitro and in vivo studies in mice ovaries and testes [35, 36]. It has been reported that IHH and DHH are co-expressed using qPCR in normal and knockout mouse ovaries [31, 37]. In mice, HH proteins are expressed in granulosa cells of primary to antral follicles [21], which is different from our results. To confirm our findings, we performed qPCR on *Ihh* in postmenopausal ovaries (52–79 years of age), which revealed *Ihh* mRNA expression in this cell population. As reported in previous studies on mouse ovaries [3, 9], GDF9 is required to trigger the HH pathway in follicles. Perhaps the presence of GDF9 in stromal cells of postmenopausal human ovaries might be the reason for *Ihh* mRNA and protein expression. IHH and DHH start to be expressed in murine

granulosa cells on day 4 after birth, when some primordial follicles have already been activated to grow to the primary stage [21]. The SHH expression pattern in mice is different from that of IHH and DHH. Levels are higher in mouse ovaries at birth, decrease by day 4, and then return to higher values in prepubertal ovaries, before declining in adult mice [21]. According to deletion studies in mice, IHH and DHH are involved in governing the differentiation and steroidogenic capacity of adrenal, theca, and Leydig cells by regulating steroidogenic enzymes [3, 10]. These results are consistent with our findings on HH expression in reproductive-age and postmenopausal ovaries. Indeed, stromal cells in reproductive-age [27, 38–40] and postmenopausal [41–44] human ovaries exhibit steroidogenic activity.

Our results on PTCH1 expression in humans differ from those of Wijgerde et al. [9], which showed that PTCH1 only appears at the primary stage of follicles in mice. On the other hand, PTCH1 expression in granulosa and theca cells from human reproductive-age ovaries is in line with what was previously reported in bovine [31] and mouse [21] follicles. The presence of PTCH1 in stromal cells could be due to the presence of previously needed markers to trigger the HH pathway in human ovaries. In mouse ovaries, Wijgerde et al. [9] reported low background mRNA levels for the *Ptch1* gene over the whole ovary, while expression of this target gene was clearly upregulated in cells surrounding follicles. PTCH1 is a key component of the HH signaling pathway, which controls cell

fate during development [45]. Expression of PTCH1 in the cytoplasm of oocytes was the same as previously observed in mouse follicles [21]. As reported by Wijgerde et al. [9], oocytes are probably exposed to IHH and DHH from surrounding granulosa cells and express the PTCH1 receptor but lack the SMO signal transducer. That is why even in the presence of the PTCH1 receptor, the HH pathway is not complete and there is no steroidogenic activity in oocytes [9]. It has been shown that although granulosa cells from antral follicles in mice produce DHH and IHH ligands, their targets, PTCH1, SMO, GLI1, GLI2, and GLI3, reside in theca, granulosa, and stromal cells [9, 21]. While our results indicate that HH ligands, PTCH1, GLI1, GLI2, and GLI3, initiate their expression in fetal ovaries of humans, in mice, the HH pathway is presumably inactive because of the absence of DHH, PTCH1, GLI1, and GLI2 expressions [10, 29], which are only activated in adult mouse ovaries [30]. The presence of GLI1, 2, and 3 proteins and *Gli3* mRNA and absence of *Gli1* and 2 mRNA in postmenopausal ovaries might be due to the lifetime of the protein and high degradation rate of mRNA, as well as a difference in the course of steroidogenesis in postmenopausal compared to reproductive-age ovaries. Human postmenopausal ovaries have a unique pattern of steroidogenic enzyme expression that favors  $\Delta^5$  steroid formation over  $\Delta^4$  steroid formation, evidenced by qPCR and Western blot analyses [44]. The presence of three different GLI proteins in vertebrates as opposed to one Ci ortholog in *Drosophila* points to more complex responses within target fields. Therefore, cellular responses to HH signaling might not just depend on levels of ligand exposure, but also particular *Gli* gene expression [17].

Based on the known role of the HH signaling pathway in cell proliferation, survival, and differentiation [46] as well as our findings, we hypothesize that HH proteins could be involved in human gonadal development and function, as in *Drosophila* [17, 46–48]. Furthermore, due to the nature of the ovary as a super-dynamic organ and its role in steroidogenesis and follicle development, it makes sense that HH proteins and their downstream targets are expressed at all ages in the human ovary. Our results also indicate that unlike in mice, GLI is expressed at all human ovary ages and could be involved in steroidogenesis as a general rather than a specific marker of theca cells.

In our study, the differences observed in human ovaries compared to mice could be due to the species' discrepancy. Studies on the development of the mouse ovary are not sufficient to understand ovarian organogenesis in humans. While in mice, it is fast and relatively more uncomplicated, lacking gonadal cords before sex differentiation, in humans, it is slow and shows a cortex with cords enclosing the germ cells and a medulla without cords. Major differences are evident in the medullary region, which is very small in mice, whereas it is evident in humans ([49], reviewed by [50]). Additionally, there are morphological variations between mouse and human ovarian

follicles from histological evaluations. Differences in follicle and oocyte diameter concerning the maturation stage, in the ratio of the follicle to oocyte diameter, and in the proliferation of follicular cells have all been shown to be specific to the species [51]. Recent studies have undertaken an extensive scRNA-seq analysis of follicle-resident and stromal cell populations in the human adult ovary [52, 53]. As efforts to provide a comprehensive atlas of cellular diversity within all organs and tissues proceed at a rapid pace, increased resolution of cell types governing human folliculogenesis is crucial, mainly because animal models are not always faithful to human reproductive processes and access to human ovarian tissue is limited [54]. A recently published study by Fan et al. [52] suggests that *NME2*, *APOD*, *APOC1*, *MEST*, *WFDC1*, *MATN2*, *PTCH1*, and *ACTA2* are markers of precursor theca cells in human ovaries. While immunostaining patterns of PTCH1 in the current study do not confirm this protein as a marker of precursor theca cells, these apparently contradictory findings nevertheless underline the fact that the human ovary is complex and subtle and that the roles of all these proteins with different lifetimes require further investigation to achieve some clarity.

While our study offers a first overview of the expression of the proteins involved in the HH signaling pathway in the human ovary, as evidenced by immunostaining, our analysis can only show the localization of these proteins in the cells. We cannot know about the host and recipient cells. This is an essential piece of information because it would allow us to understand where the proteins are produced and to where they migrate and are expressed. To this end, in situ hybridization studies are recommended to complete our findings [26, 27]. To disregard PTCH and GLI as specific markers for precursor theca cells, in situ hybridization could be a promising technique to be applied to co-localize the mentioned markers and gene products associated with steroidogenesis. However, it is important to bear in mind that our previous findings showed that not all ovarian cells could differentiate into theca cells [28], which does not corroborate with our current results showing that PTCH and GLI are expressed all over the ovarian stromal tissue.

Our findings on the GDF9-HH-GLI pathway provide a foundation for future investigations into human ovaries. They could be applied to define cell-specific responses to GDF9-HH-GLI signaling in human follicles and stromal cells, determining how this pathway modulates follicle development and steroidogenic function in ovaries from the fetal to the postmenopausal stage.

**Supplementary Information** The online version contains supplementary material available at <https://doi.org/10.1007/s10815-021-02161-w>.

**Acknowledgements** We are grateful to Mira Hryniuk, BA, for reviewing the English language of the manuscript and Dolores Gonzalez and Olivier Van Kerk for their technical assistance.

**Author contribution** P. A.: study design, experimental procedures, analysis, interpretation of data, and manuscript preparation. C. D.: experimental procedures and analysis. M. M. D.: manuscript revision. E. M.: tissue supply, analysis of IHC staining, and manuscript revision. A. C.: tissue supply. C. A. A.: experimental design, experimental procedures, interpretation of results, and manuscript revision.

**Funding** This study was supported by grants from the Fonds National de la Recherche Scientifique de Belgique (FNRS) (C. A. Amorim is an FRS-FNRS Research Associate; grant MIS #F4535 16 awarded to C. A. Amorim; grant 5/4/150/5 awarded to M. M. Dolmans; grant ASP-RE314 awarded to P. Asiabi) and the Fondation Contre le Cancer (grant 2018-042 awarded to A. Camboni).

## Declarations

**Conflict of interest** The authors declare no competing interests.

## References

- Edson MA, Nagaraja AK, Matzuk MM. The mammalian ovary from genesis to revelation. *Endocr Rev*. 2009;30(6):624–712.
- Matzuk MM, Lamb DJ. The biology of infertility: research advances and clinical challenges. *Nat Med*. 2008;14(11):1197–213.
- Liu C, Peng J, Matzuk MM, Yao HH-C. Lineage specification of ovarian theca cells requires multicellular interactions via oocyte and granulosa cells. *Nat Commun*. 2015;6(1):1–11.
- Lapointe E, Boerboom D. WNT signaling and the regulation of ovarian steroidogenesis. *Front Biosci* (Scholar ed). 2011;3:276–85.
- Honda A, Hirose M, Hara K, Matoba S, Inoue K, Miki H, et al. Isolation, characterization, and in vitro and in vivo differentiation of putative thecal stem cells. *PNAS*. 2007;104(30):12389–94.
- Dong J, Albertini DF, Nishimori K, Kumar TR, Lu N, Matzuk MM. Growth differentiation factor-9 is required during early ovarian folliculogenesis. *Nature*. 1996;383(6600):531–5.
- Varjosalo M, Taipale J. Hedgehog: functions and mechanisms. *Genes Dev*. 2008;22(18):2454–72.
- Liu C-F, Liu C, Yao HH-C. Building pathways for ovary organogenesis in the mouse embryo. In: *Current topics in developmental biology*, vol. 90. Amsterdam: Elsevier; 2010. p. 263–90.
- Wijgerde M, Ooms M, Hoogerbrugge JW, Grootegoed JA. Hedgehog signaling in mouse ovary: Indian hedgehog and desert hedgehog from granulosa cells induce target gene expression in developing theca cells. *Endocrinology*. 2005;146(8):3558–66.
- Yao HH-C, Whoriskey W, Capel B. Desert hedgehog/patched 1 signaling specifies fetal Leydig cell fate in testis organogenesis. *Genes Dev*. 2002;16(11):1433–40.
- Richards JS, Ren YA, Candelaria N, Adams JE, Rajkovic A. Ovarian follicular theca cell recruitment, differentiation, and impact on fertility: 2017 update. *Endocr Rev*. 2017;39(1):1–20.
- Marion G, Gier H, Choudary J. Micromorphology of the bovine ovarian follicular system. *J Anim Sci*. 1968;27(2):451–65.
- Stone DM, Hynes M, Armanini M, Swanson TA, Gu Q, Johnson RL, et al. The tumour-suppressor gene patched encodes a candidate receptor for Sonic hedgehog. *Nature*. 1996;384(6605):129–34.
- Fuse N, Maiti T, Wang B, Porter JA, Hall TMT, Leahy DJ, et al. Sonic hedgehog protein signals not as a hydrolytic enzyme but as an apparent ligand for patched. *Proc Natl Acad Sci*. 1999;96(20):10992–9.
- Ingham P, Taylor A, Nakano Y. Role of the *Drosophila* patched gene in positional signalling. *Nature*. 1991;353(6340):184–7.
- Taipale J, Cooper M, Maiti T, Beachy P. Patched acts catalytically to suppress the activity of Smoothened. *Nature*. 2002;418(6900):892–6.
- Ingham PW, McMahon AP. Hedgehog signaling in animal development: paradigms and principles. *Genes Dev*. 2001;15(23):3059–87.
- Gulino A, Di Marcotullio L, Ferretti E, De Smaele E, Screpanti I. Hedgehog signaling pathway in neural development and disease. *Psychoneuroendocrinology*. 2007;32:S52–S6.
- Di Marcotullio L, Ferretti E, Greco A, De Smaele E, Screpanti I, Gulino A. Multiple ubiquitin-dependent processing pathways regulate hedgehog/gli signaling: implications for cell development and tumorigenesis. *Cell Cycle*. 2007;6(4):390–3.
- Lum L, Beachy PA. The Hedgehog response network: sensors, switches, and routers. *Science*. 2004;304(5678):1755–9.
- Russell MC, Cowan RG, Harman RM, Walker AL, Quirk SM. The hedgehog signaling pathway in the mouse ovary. *Biol Reprod*. 2007;77(2):226–36.
- Asiabi P, Ambroise J, Giachini C, Coccia ME, Bearzatto B, Chiti MC, et al. Assessing and validating housekeeping genes in normal, cancerous, and polycystic human ovaries. *J Assist Reprod Genet*. 2020. <https://doi.org/10.1007/s10815-020-01901-8>.
- Young J, McNeilly AS. Theca: the forgotten cell of the ovarian follicle. *Reproduction*. 2010;140(4):489–504.
- Magoffin DA, Magarelli PC. Preantral follicles stimulate luteinizing hormone independent differentiation of ovarian theca-interstitial cells by an intrafollicular paracrine mechanism. *Endocr Rev*. 1995;3(2):107–12.
- Magoffin DA. Ovarian theca cell. *Int J Biochem Cell Biol*. 2005;37(7):1344–9.
- Orisaka M, Tajima K, Mizutani T, Miyamoto K, Tsang BK, Fukuda S, et al. Granulosa cells promote differentiation of cortical stromal cells into theca cells in the bovine ovary. *Biol Reprod*. 2006;75(5):734–40.
- Qiu M, Quan F, Han C, Wu B, Liu J, Yang Z, et al. Effects of granulosa cells on steroidogenesis, proliferation and apoptosis of stromal cells and theca cells derived from the goat ovary. *J Steroid Biochem Mol Biol*. 2013;138:325–33.
- Asiabi P, Dolmans M, Ambroise J, Camboni A, Amorim C. In vitro differentiation of theca cells from ovarian cells isolated from postmenopausal women. *Hum Reprod*. 2020;35(12):2793–807.
- Bitgood MJ, McMahon AP. Hedgehog and Bmp genes are coexpressed at many diverse sites of cell-cell interaction in the mouse embryo. *Develop Biol*. 1995;172:126.
- Huang CCJ, Yao HHC. Diverse functions of Hedgehog signaling in formation and physiology of steroidogenic organs. *Mol Reprod Dev Incorpor Gamete Res*. 2010;77(6):489–96.
- Spicer LJ, Sudo S, Aad PY, Wang LS, Chun S-Y, Ben-Shlomo I, et al. The hedgehog-patched signaling pathway and function in the mammalian ovary: a novel role for hedgehog proteins in stimulating proliferation and steroidogenesis of theca cells. *Reproduction*. 2009;138(2):329–39.
- Otsuka F, McTavish KJ, Shimasaki S. Integral role of GDF-9 and BMP-15 in ovarian function. *Mol Reprod Dev*. 2011;78(1):9–21.
- Sun R, Lei L, Cheng L, Jin Z, Zu S, Shan Z, et al. Expression of GDF-9, BMP-15 and their receptors in mammalian ovary follicles. *J Mol Histol*. 2010;41(6):325–32.
- Riepsamen AH, Chan K, Lien S, Sweeten P, Donoghoe MW, Walker G, et al. Serum concentrations of oocyte-secreted factors BMP15 and GDF9 during IVF and in women with reproductive pathologies. *Endocrinology*. 2019;160(10):2298–313.
- Echelard Y, Epstein DJ, St-Jacques B, Shen L, Mohler J, McMahon JA, et al. Sonic hedgehog, a member of a family of putative signaling molecules, is implicated in the regulation of CNS polarity. *Cell*. 1993;75(7):1417–30.



36. Bitgood MJ, Shen L, McMahon AP. Sertoli cell signaling by Desert hedgehog regulates the male germline. *Curr Biol*. 1996;6(3):298–304.
37. Van Den Brink GR, Bleuming SA, Hardwick JC, Schepman BL, Offerhaus GJ, Keller JJ, et al. Indian Hedgehog is an antagonist of Wnt signaling in colonic epithelial cell differentiation. *Nat Genet*. 2004;36(3):277–82.
38. Parikh G, Varadinova M, Suwandhi P, Araki T, Rosenwaks Z, Poretsky L, et al. Vitamin D regulates steroidogenesis and insulin-like growth factor binding protein-1 (IGFBP-1) production in human ovarian cells. *Horm Metab Res*. 2010;42(10):754–7.
39. Channing CP. Steroidogenesis and morphology of human ovarian cell types in tissue culture. *J Endocrinol*. 1969;45(2):297–NP.
40. Qiu M, Liu J, Han C, Wu B, Yang Z, Su F, et al. The influence of ovarian stromal/theca cells during in vitro culture on steroidogenesis, proliferation and apoptosis of granulosa cells derived from the goat ovary. *Reprod Domest Anim*. 2014;49(1):170–6.
41. Fogle RH, Stanczyk FZ, Zhang X, Paulson RJ. Ovarian androgen production in postmenopausal women. *J Clin Endocrinol Metab*. 2007;92(8):3040–3.
42. Couzinet B, Meduri G, Lecce MG, Young J, Brailly S, Loosfelt H, et al. The postmenopausal ovary is not a major androgen-producing gland. *J Clin Endocrinol Metab*. 2001;86(10):5060–6.
43. Dupont E, Labrie F, Luu-The V, Pelletier G. Immunocytochemical localization of 3 beta-hydroxysteroid dehydrogenase/delta 5-delta 4-isomerase in human ovary. *J Clin Endocrinol Metab*. 1992;74(5):994–8.
44. Havelock JC, Rainey WE, Bradshaw KD, Carr BR. The postmenopausal ovary displays a unique pattern of steroidogenic enzyme expression. *Hum Reprod*. 2005;21(1):309–17.
45. Hammerschmidt M, Brook A, McMahon AP. The world according to hedgehog. *Trends Genet*. 1997;13(1):14–21.
46. Walterhouse DO, Lamm ML, Villavicencio E, Iannaccone PM. Emerging roles for hedgehog-patched-Gli signal transduction in reproduction. *Biol Reprod*. 2003;69(1):8–14.
47. Nüsslein-Volhard C, Wieschaus E. Mutations affecting segment number and polarity in *Drosophila*. *Nature*. 1980;287(5785):795–801.
48. McMahon AP, Ingham PW, Tabin CJ. 1 Developmental roles and clinical significance of Hedgehog signaling. *Curr Top Dev Biol*. 2003;53:1–114.
49. Mara H. Rendi, Atis Muehlenbachs, Rochelle L. Garcia, Kelli L. Boyd. 17 - Female Reproductive System. In: Piper M. Treuting, Dintzis SM, editors. *Comparative Anatomy and Histology* Cambridge: Academic Press; 2012. p. 253–284.
50. Jimenez R. Ovarian organogenesis in mammals: mice cannot tell us everything. *Sex Dev*. 2009;3(6):291–301.
51. Griffin J, Emery BR, Huang I, Peterson CM, Carrell DT. Comparative analysis of follicle morphology and oocyte diameter in four mammalian species (mouse, hamster, pig, and human). *J Exper Clin Assist Reprod*. 2006;3(1):1–9.
52. Fan X, Bialecka M, Moustakas I, Lam E, Torrens-Juaneda V, Borggreven N, et al. Single-cell reconstruction of follicular remodeling in the human adult ovary. *Nat Commun*. 2019;10(1):1–13.
53. Wagner M, Yoshihara M, Douagi I, Damdimopoulos A, Panula S, Petropoulos S, et al. Single-cell analysis of human ovarian cortex identifies distinct cell populations but no oogonial stem cells. *Nat Commun*. 2020;11(1):1147–62.
54. Man L, Lustgarten-Guahmich N, Kallinos E, Redhead-Laconte Z, Liu S, Schattman B, et al. Comparison of human antral follicles of xenograft versus ovarian origin reveals disparate molecular signatures. *Cell Rep*. 2020;32(6):108027.

**Publisher's note** Springer Nature remains neutral with regard to jurisdictional claims in published maps and institutional affiliations.